

UCLA

UCLA Previously Published Works

Title

Preparation and stability of pegylated poly(S-alkyl-L-homocysteine) coacervate core micelles in aqueous media

Permalink

<https://escholarship.org/uc/item/224274gk>

Journal

The European Physical Journal E, 46(9)

ISSN

1292-8941

Authors

Benavides, Isaac

Scott, Wendell A

Cai, Xiaoying

et al.

Publication Date

2023-09-01

DOI

10.1140/epje/s10189-023-00339-x

Peer reviewed

Preparation and stability of pegylated poly(S-alkyl-L-homocysteine) coacervate core micelles in aqueous media

Isaac Benavides^{a†}, Wendell A. Scott^{a†}, Xiaoying Cai^b, Z. Hong Zhou^{b,c}, Timothy J. Deming^{a,c,d*}

^a Department of Chemistry and Biochemistry, University of California, Los Angeles, CA 90095, USA

^b Department of Microbiology, Immunology and Molecular Genetics, University of California, Los Angeles, Los Angeles, CA 90095

^c California NanoSystems Institute, University of California, Los Angeles, CA 90095

^d Department of Bioengineering, University of California, Los Angeles, CA 90095, USA

† These authors contributed equally

Corresponding Author

* demingt@seas.ucla.edu

ORCID

Timothy J. Deming: 0000-0002-0594-5025

Abstract

We report development and preparation of synthetic polypeptide based, coacervate core polyelectrolyte complex micelles, PCMs, in aqueous media, which were characterized and evaluated for the encapsulation and *in vitro* release of a model single-stranded RNA, polyadenylic acid, poly(A). Cationic, α -helical polypeptides pegylated at their N-termini, **PEG₁₁₃-b-5b_n** and **PEG₁₁₃-b-5c_n**, were designed to form coacervate core PCMs upon mixing

with multivalent anions in aqueous media. Sodium tripolyphosphate (TPP) and poly(A) were used as model multivalent anions that allowed optimization of polypeptide composition and chain length for formation of stable, nanoscale PCMs. **PEG₁₁₃-b-5c₂₇** was selected for preparation of PCMs that were characterized under different environmental conditions using dynamic light scattering, atomic force microscopy and cryoelectron microscopy. The PCMs were found to efficiently encapsulate poly(A), were stable at physiologically relevant pH and solution ionic strength, and were able to release poly(A) in the presence of excess polyvalent anions. These PCMs were found to be a promising model system for further development of polypeptide based therapeutic delivery vehicles.

1. Introduction

In recent years, the delivery of biologics such as proteins and polynucleotides has become increasingly important in the pharmaceutical industry. Biologics are an attractive alternative to small molecule drugs due to their high potency and specificity [1]. With the discovery of DNA came the first conceived uses of therapeutic polynucleotides for the replacement of defective genetic material [2,3]. In addition to the use of plasmid DNA (pDNA) for gene therapy, the area of polynucleotide-based therapeutics has expanded to include messenger RNA (mRNA), small interfering RNA (siRNA), micro RNA (miRNA), and antisense oligonucleotides (ASO) [4-6].

When administered alone, these mechanistically diverse polynucleotide therapeutics are all vulnerable to degradation and have difficulty entering cells [4-6]. Chemical modifications to the nucleotide backbone can remedy some of these problems but can also increase the prevalence of off-target effects. Alternative approaches involve encapsulation of polynucleotides within viral capsid vehicles [7] or in non-viral vehicles such as lipid nanoparticles [8] or polyelectrolyte complexes (PEC), sometimes referred to as polyplexes [9]. These encapsulation strategies increase polynucleotide circulation lifetime and aid in cell internalization, but they often require complex formulations that can cause significant adverse side effects [10,11].

Polyvalent cations are required for the formation of PECs with anionic polynucleotides. The formation of PECs in aqueous media is primarily driven by an entropic gain from the release of bound counterions that were associated with the multiple charged residues along the polymeric chains [12,13]. When PEC formation results in liquid-liquid phase separation in aqueous media, the products are called complex coacervates (CCs) [14]. In general, CCs are sensitive to the pH and ionic strength of the aqueous media [15–17], possess low interfacial surface tension [18,19], and have the ability to stabilize their cargos against degradation [20,21], which makes them potentially valuable for polynucleotide delivery applications.

Due to their generally good biocompatibility and biodegradability, cationic synthetic polypeptides have been used to form PECs for polynucleotide delivery [22–26]. The most widely used polypeptides include poly(L-lysine), poly(L-arginine), and poly(L-ornithine) [27,28]. However, these cationic polypeptides based on natural amino acids possess chemical functionality that is not optimal for polynucleotide delivery. To improve delivery efficacy, it would be desirable to have polypeptides with tunable features such as the pK_a s of charged groups, chain conformations, and hydrophobicity. accordingly, both poly(L-lysine) and poly(L-glutamate) have been chemically modified at their side-chain groups to alter physicochemical properties and enhance the delivery of polynucleotides. Modification of primary amine side-chains of poly(L-lysine) or carboxylate side-chains of poly(L-glutamate) [29–31] offer a means to add ligands [32], hydrophobic groups [33], thiols [34], and imidazole moieties [35]. These modifications have been used to alter PEC properties such as targeting capabilities, PEC stability, and enhance endosomal escape. However, these approaches typically only adjust a single feature at a time. While multiple modifications can be used to optimize a variety of features, modification of different peptide residues in different ways results in compositional heterogeneity that complicates both molecular understanding and downstream regulatory pathways.

Another widely used strategy to improve polypeptide mediated delivery of polynucleotides is the incorporation of polyethylene glycol (PEG) as a non-ionic hydrophilic segment in dual hydrophilic PEG-polypeptide block copolymers. For clinical applications, there are known disadvantages for the use of PEG based materials for therapeutic delivery, including rapid clearance from the blood stream and allergic reactions [36,37], yet PEG is useful for proof of concept studies aimed at understanding assembly and structures in the development of new PEC materials. Incorporating PEG segments into one [38] or both [39] PEC components has been found to result in formation of polyelectrolyte complex micelles, PCMs, that are stabilized against aggregation and coalescence by the PEG chains. The size of these assemblies is dependent on the ratio of the PEG segments to the charged segments and thus can be controlled by varying copolymer compositions [40–42]. Additionally, different nanoscale PCM morphologies can be obtained by variation of the polynucleotide component (i.e. single-stranded or double-stranded) [29,43–45]. Structural differences result from differences in chain packing in the micelle cores, which can range from ordered solids to liquid coacervates [45,46]. There are many examples of PEG-polypeptide-based PCMs for delivery of polynucleotides such as pDNA [47,48], siRNA [49,50], and ASOs [51], which supports the potential utility of the PCM approach in our model system.

Here, we designed new double hydrophilic block copolymers of PEG and amino acid functionalized, cationic α -helical polypeptides to enable formation of coacervate core PCMs upon mixture with multivalent anions in aqueous media. We sought to improve upon the PCM approach by incorporating recently developed multifunctional cationic polypeptides that we have shown form coacervates with multivalent ions, and possess many adjustable side-chain molecular features that can be used to alter their properties in response to physiologically relevant changes in pH, temperature, and redox [52]. The goals of this study were to determine copolymer compositions that were effective in

forming coacervate core PCMs, and to characterize them and evaluate their properties in aqueous media.

2. Results and Discussion

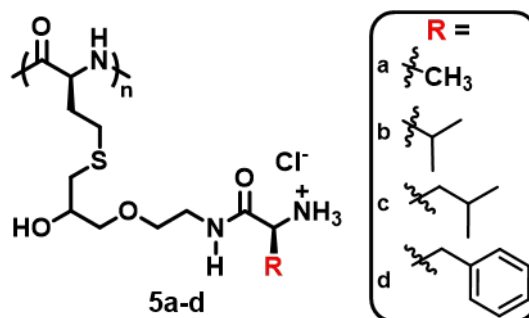


Figure 1 Structures of cationic, α -helical polypeptides **5a-d**.

Our group has developed a highly versatile, modular reaction for conversion of poly(L-methionine), **M** into side-chain functionalized poly(S-alkyl-L-homocysteine) derivatives that possess stable α -helical conformations [53,54]. We recently employed this methodology to prepare a series of cationic poly(S-alkyl-L-homocysteine)s containing hydrophobic amino acids in their side-chains, **5a-5d**, which were found to undergo liquid-liquid phase separation in aqueous media upon mixing with oppositely charged multivalent anions (Figure 1) [52]. We found that use of different side-chain amino acids allowed physiologically relevant tuning of coacervate formation in response to variation of solution pH, temperature, ionic strength, and counterion valency. While our previous work introduced these cationic, α -helical polypeptides as a model system to study molecular features that promote polypeptide coacervation, this study was focused on using these coacervate forming polypeptide segments to prepare stable nanoscale PCMs for potential downstream applications in polynucleotide delivery. Here, we designed and prepared different compositions of PEG-poly(S-alkyl-L-homocysteine) block copolymers, **PEG₁₁₃-b-5b_n** and **PEG₁₁₃-b-5c_n** (Figure 2), to study formation and stability of PCMs in the presence of model multivalent anions [55].

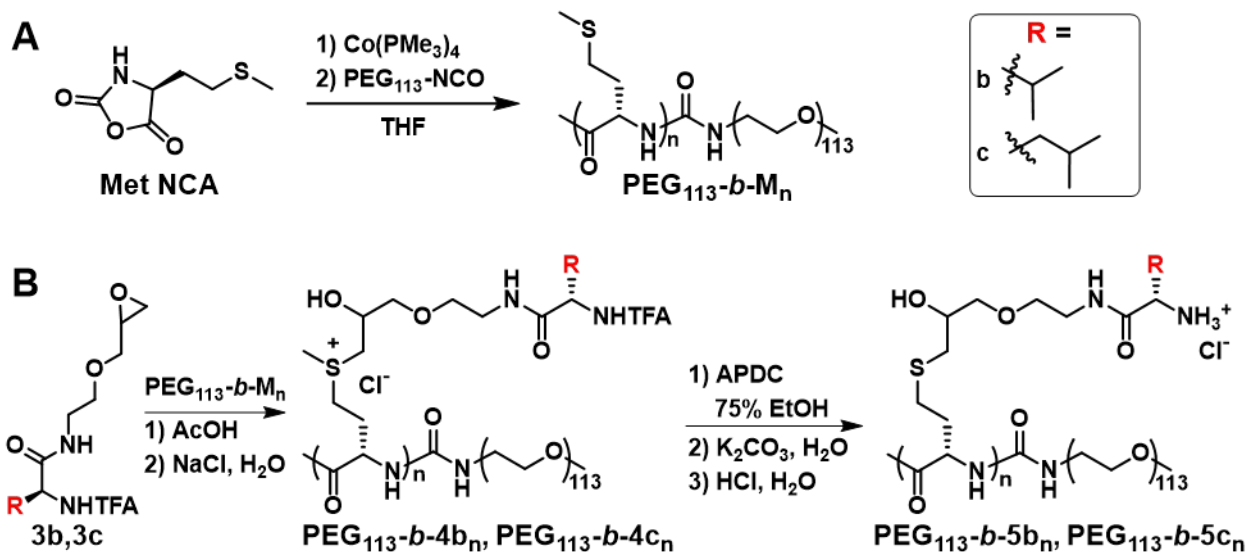


Figure 2 (A) Synthesis of PEG₁₁₃-b-M_n copolymers. (B) Synthesis of PEG₁₁₃-b-5b_n and PEG₁₁₃-b-5c_n copolymers and intermediates. n = 27 or 51.

To prepare the desired block copolymers, **M** chains with average degrees of polymerization (DP) of 27 and 51 were synthesized using established methods for the living ring-opening polymerization of L-methionine N-carboxyanhydride (Met NCA) [56]. These active chains were both end-capped with α -methoxy- ω -isocyanoethyl-poly(ethylene glycol)₁₁₃ (PEG₁₁₃-NCO) to give PEG₁₁₃-b-M₂₇ and PEG₁₁₃-b-M₅₁ (Figure 2). These block copolymers were then each separately functionalized with epoxides **3b** or **3c** followed by demethylation and deprotection steps to provide the four desired final block copolymers: PEG₁₁₃-b-5b₂₇, PEG₁₁₃-b-5c₂₇, PEG₁₁₃-b-5b₅₁, and PEG₁₁₃-b-5c₅₁ (Figure 2) [52–54]. These copolymers were isolated as hydrochloride salts in high yields (see supplemental information (SI): Table S1), and quantitative modification of methionine residues was verified via ¹H NMR characterization (see SI). These copolymer compositions were selected based on the properties of **5b** and **5c** homopolypeptides, which possess good aqueous solubility and had been found to form coacervates with multivalent anions under physiologically relevant conditions [57–59].

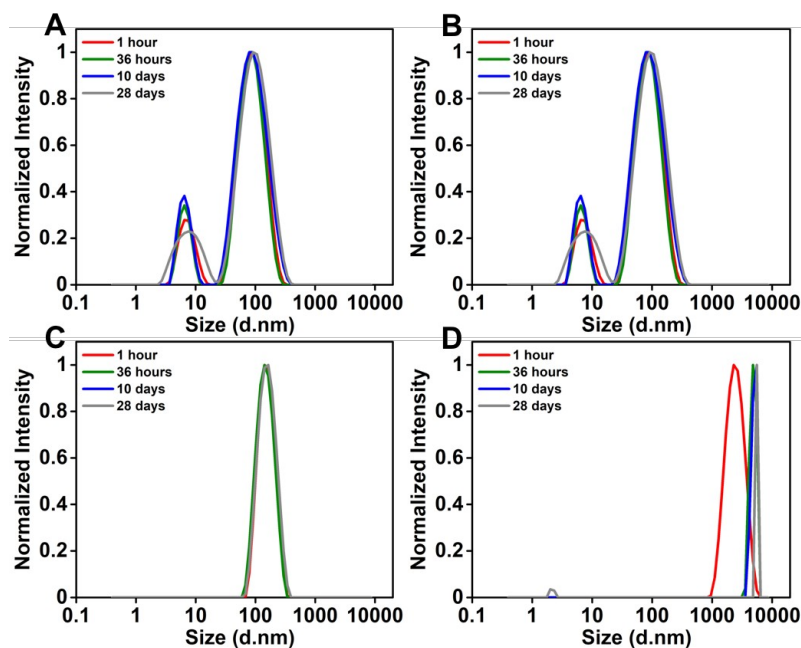


Figure 3 Normalized intensity size distributions of TPP-PCM suspensions over time from DLS analysis. Suspensions of TPP-PCMs were prepared from (A) **PEG₁₁₃-b-5b₂₇**, (B) **PEG₁₁₃-b-5b₅₁**, (C) **PEG₁₁₃-b-5c₂₇**, and (D) **PEG₁₁₃-b-5c₅₁** (all at 5 mg/mL) in water containing 13 mM TPP and 150 mM NaCl at 20 °C. d.nm = average hydrodynamic diameter in nanometers.

Time After Preparation	Hydrodynamic diameter (intensity distribution, nm)			
	PEG ₁₁₃ -b-5b ₂₇	PEG ₁₁₃ -b-5c ₂₇	PEG ₁₁₃ -b-5b ₅₁	PEG ₁₁₃ -b-5c ₅₁
1 hour	7.5 ± 15; 97 ± 45	160 ± 49	7.9 ± 3.4; 140 ± 66	2500 ± 880
36 hours	6.7 ± 1.6; 94 ± 42	150 ± 49	8.0 ± 3.5; 160 ± 80	4900 ± 560
10 days	6.7 ± 1.7; 100 ± 55	170 ± 55	8.1 ± 3.3; 150 ± 72	5100 ± 510
28 days	110 ± 58	170 ± 61	140 ± 67	5600 ± 610

Table

1 Hydrodynamic diameters of TPP-PCM suspensions determined from DLS intensity distributions. Suspensions of TPP-PCMs were prepared from different copolymers (all at 5.0 mg/mL) in in water containing 13 mM TPP and 150 mM NaCl at 20 °C.

The four block copolymers were evaluated to identify the best composition able to form uniform populations of nanoscale PCMs that are stable in aqueous media. For initial studies, sodium triphosphate (TPP) was used as a model multivalent anion that is known to form coacervates when mixed with either homopolymer **5b** or **5c** [52]. In the presence of 13 mM TPP in deionized (DI) water, all four copolymers were found form TPP-polyelectrolyte complex micelles (TPP-PCMs). Using dynamic light scattering (DLS) to monitor hydrodynamic diameter of the resulting assemblies, we found that both **PEG₁₁₃-b-5b₂₇** and **PEG₁₁₃-b-5b₅₁** formed multimodal particle size distributions (Figure 3a-b, Table 1) with significant populations of copolymer unimers (see SI: Figure S1, and Table S2). Initially, both **PEG₁₁₃-b-5c₂₇** and **PEG₁₁₃-b-5c₅₁** formed TPP-PCMs with monomodal size distributions (Figure 3c-d, and Table 1), although the larger **PEG₁₁₃-b-5c₅₁** TPP-PCMs were observed to settle over time leaving behind only copolymer unimers in solution (see SI: Figure S1, and Table S2). In contrast, the **PEG₁₁₃-b-5c₂₇** TPP-PCMs remained suspended for up to 28 days (see SI: Figure S1, and Table S2). The inability of the **PEG₁₁₃-b-5c₅₁** TPP-PCMs to remain colloidally stable over the 28 day period was likely due to coalescence of smaller PCMs into larger droplets, which was confirmed by optical microscopy (Figure 4a). Based on these results, the TPP-PCMs prepared with **PEG₁₁₃-b-5c₂₇** were found to be optimal for formation of stable, uniform nanoscale PCMs as confirmed by DLS (Figure 3c, Table 1) and atomic force microscopy (AFM) imaging (Figure 4b).

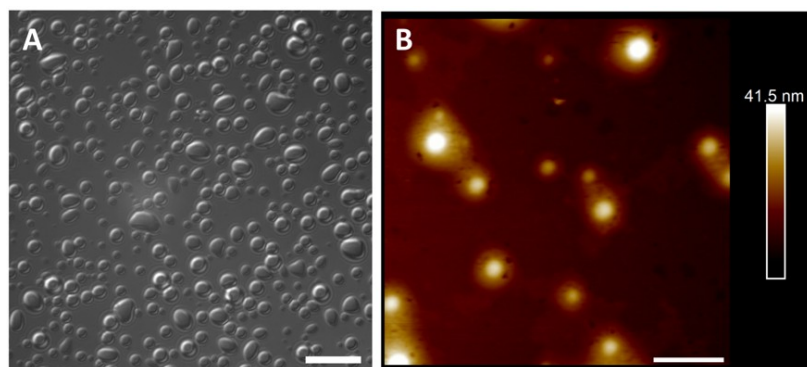


Figure 4 Imaging of TPP-PCMs prepared with **PEG₁₁₃-b-5c_n**. (A) Optical micrograph of TPP-PCMs prepared with **PEG₁₁₃-b-5c₅₁** (5.0 mg/mL) in water containing 13 mM TPP and 150

mM NaCl at 20 °C. The suspension was aged 1 hour and allowed to settle before imaging. Scale bar = 20 μ m. (B) AFM topography image of TPP-PCMs prepared with **PEG₁₁₃-b-5c₂₇** (5.0 mg/mL) in water containing 13 mM TPP and 150 mM NaCl at 20 °C. The suspension was aged 1 hour, diluted with nuclease-free water to a final copolymer concentration of 0.1 mg/mL and then dropcast onto a freshly cleaved mica surface and allowed to dry. Scale bar = 400 nm; vertical scale range: 0 to 41.5 nm.

We next sought to determine how **PEG₁₁₃-b-5c_n** copolymers behaved when complexed with single-stranded RNA (ssRNA) in aqueous media. The selection of ssRNA as a model genetic payload was due to the propensity of flexible single-stranded oligonucleotides to form CCs as opposed to ordered solid PECs, and since we had previously observed that ssRNA forms a CC with homopolymer **5c** [43,52,60]. We focused on the **PEG₁₁₃-b-5c_n** copolymers due to their successful formation of TPP-PCMs, and poly(A) was used as a model sequence to form ssRNA containing PCMs. When aqueous solutions of poly(A) were mixed with solutions of **PEG₁₁₃-b-5c_n** at equimolar charge ratios, the mixtures immediately became turbid, indicative of PCM formation. To evaluate hydrodynamic diameter and stability of the assemblies, the suspensions of poly(A)-polyelectrolyte complex micelles (poly(A)-PCMs) were analyzed using DLS over 16 days. The poly(A)-PCMs prepared with **PEG₁₁₃-b-5c₂₇** were found to possess an average hydrodynamic diameter of 107 ± 26 nm at one hour and were stable against coalescence over the duration of the experiment (Figure 5a, see SI: Figure S2, and Tables S3,S4). In comparison, the poly(A)-PCMs prepared with **PEG₁₁₃-b-5c₅₁** possessed broad size distributions that changed over the course of the study (Figure 5b, see SI: Figure S2, and Tables S3,S4). To confirm formation of spherical micelles, poly(A)-PCMs prepared with **PEG₁₁₃-b-5c₂₇** were further characterized using AFM and cryoelectron microscopy (cryoEM) (Figure 5c,d). Both imaging techniques showed the presence of spherical particles with sizes comparable to the size distributions observed by DLS. Based on these

results, we selected the nanoscale poly(A)-PCMs prepared with **PEG₁₁₃-b-5c₂₇** for additional studies.

To further characterize poly(A)-PCMs, their efficiency of poly(A) encapsulation was measured using RyboGreen, a fluorescent probe that binds to free, uncomplexed ssRNA. When RyboGreen was added to an aqueous suspension of poly(A)-PCMs, the resulting fluorescence signal was substantially diminished compared to the fluorescence of an aqueous solution containing a mixture of RyboGreen and free poly(A) (see SI: Figure S3). The low fluorescence of poly(A)-PCMs was due to the inability of RyboGreen to bind to the complexed poly(A), which allowed us to quantify poly(A) encapsulation and release in poly(A)-PCMs over time. Aqueous suspensions of poly(A)-PCMs were mixed with RyboGreen and then centrifuged to pellet the poly(A)-PCMs. The fluorescence signals of the supernatants, which contain any free poly(A), were then measured and compared to a calibration curve of RyboGreen complexed with known concentrations of poly(A) (see SI: Figure S4). This method provided a means to determine the concentration of free poly(A) in poly(A)-PCM samples, and revealed that *ca.* 95% of all poly(A) was encapsulated and remained within poly(A)-PCMs over a 24 hour period (see SI: Figure S3).

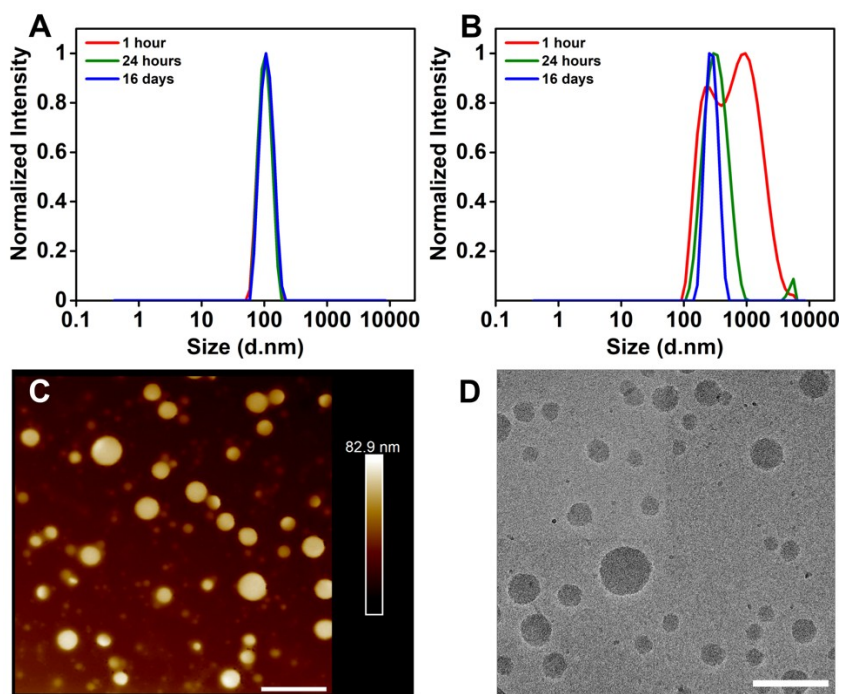


Figure 5 Normalized intensity size distributions over time and imaging of poly(A)-PCM suspensions. Suspensions of poly(A)-PCMs were prepared with (A) **PEG₁₁₃-b-5c₂₇** and (B) **PEG₁₁₃-b-5c₅₁** (both at 5.0 mg/mL) and an equimolar charge ratio of poly(A) in nuclease-free water containing 150 mM NaCl at 20 °C. d.nm = average hydrodynamic diameter in nanometers. (C) AFM topography image of a suspension of poly(A)-PCMs prepared with **PEG₁₁₃-b-5c₂₇** (1.0 mg/mL) and an equimolar charge ratio of poly(A) in nuclease-free water containing 150 mM NaCl at 20 °C. The suspension was aged for 1 hour, diluted tenfold in nuclease-free water and then dropcast onto a freshly cleaved mica surface and allowed to dry. Scale bar = 410 nm; vertical scale range: 0 to 82.9 nm. (D) CryoEM Image of a suspension of poly(A)-PCMs prepared with **PEG₁₁₃-b-5c₂₇** (25 mg/mL) and an equimolar charge ratio of poly(A) in nuclease-free water containing 150 mM NaCl at 20 °C. The suspension was aged for 1 hour and then diluted tenfold in nuclease-free water before vitrification and imaging. Scale bar = 200 nm.

Since PCMs are known to be sensitive to and can dissociate in high ionic strength aqueous media, the effects of increasing salt concentrations on poly(A)-PCM stability were studied [38,42,59,61,62]. To study changes in PCM size, hydrodynamic diameters of **PEG₁₁₃-b-5c₂₇** based poly(A)-PCMs were monitored using DLS over a range of NaCl concentrations in water. Suspensions of poly(A)-PCMs were prepared in aqueous solutions ranging from 0 to 1.0 M NaCl and allowed to stand for 1 hour before analysis (Figure 6a). We observed that poly(A)-PCM size gradually increased with increasing ionic strength in the range of *ca.* 75 mM to 350 mM NaCl (Figure 6a). At NaCl concentrations greater than *ca.* 350 mM poly(A)-PCM size was found to increase dramatically and assemblies eventually were over 5 μ m in diameter at 1.0 M NaCl (Figure 6a). The large increases in poly(A)-PCM size at high salt concentrations are generally consistent with results reported for other PCM systems [42,59,62], and are likely due to decreased aqueous solubility of PEG segments at high ionic strength, which leads to aggregation of PCMs [42]. Despite

large increases in size at high ionic strength, the poly(A)-PCMs were found to be stable at physiological ionic strength, which is relevant for potential therapeutic applications.

In addition to poly(A)-PCM size stability, we also measured how increased solution ionic strength affected the encapsulation of poly(A) cargo. Three suspensions of **PEG₁₁₃-b-5c₂₇** based poly(A)-PCMs were prepared in 150 mM NaCl and then separately diluted tenfold into aqueous 0.15 M, 0.50 M and 1.0 M NaCl. Using the RyboGreen assay, the presence of any free poly(A) in solution for these samples was quantified at zero, one, and four hours as described above. Our intent was to determine if the changes seen above in poly(A)-PCM size with increasing salt concentration were correlated with release of poly(A) cargo. Despite significant changes in poly(A)-PCM size (Figure 6a), the total amount of poly(A) released in up to 1.0 M NaCl after four hours was found to be less than 10% (Figure 6b), which suggests that changes in poly(A)-PCM size are not correlated with loss of poly(A) from the complexes, consistent with the hypothesis provided above that the PCMs primarily aggregate at high ionic strength.

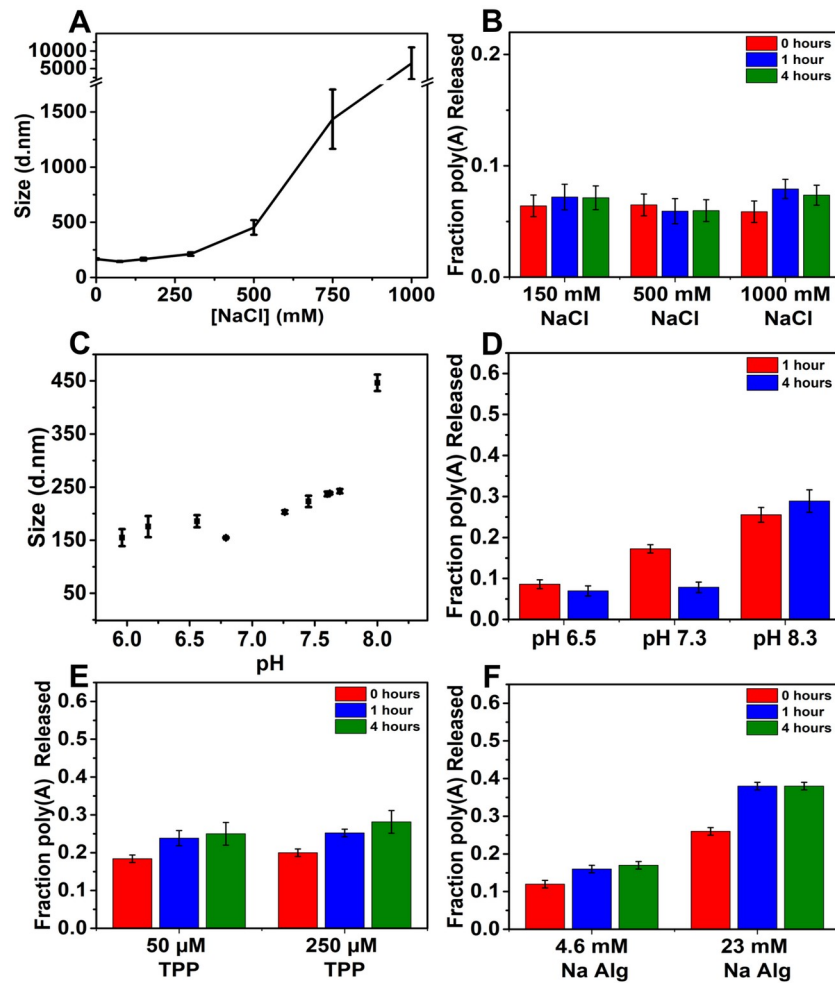


Figure 6 Stability of poly(A)-PCMs under different environmental conditions. (A) Normalized intensity size distributions of suspensions of poly(A)-PCMs prepared with **PEG₁₁₃-b-5c₂₇** (1.0 mg/mL) and an equimolar charge ratio of poly(A) in nuclease-free water at different NaCl concentrations. (B) Fraction of total poly(A) released from poly(A)-PCMs prepared with **PEG₁₁₃-b-5c₂₇** (0.1 mg/mL) and an equimolar charge ratio of poly(A) in nuclease-free water at different NaCl concentrations. (C) Normalized intensity size distributions of suspensions of poly(A)-PCMs prepared with **PEG₁₁₃-b-5c₂₇** (1.0 mg/mL) and an equimolar charge ratio of poly(A) in nuclease-free water containing 150 mM PBS at different pH. (D) Fraction of total poly(A) released from poly(A)-PCMs prepared with **PEG₁₁₃-b-5c₂₇** (0.1 mg/mL) and an equimolar charge ratio of poly(A) in nuclease-free water containing 150 mM PBS at different pH. (E,F) Fraction of total poly(A) released from poly(A)-PCMs prepared with **PEG₁₁₃-b-5c₂₇** (0.1 mg/mL) and an equimolar charge ratio of

poly(A) in nuclease-free water containing 150 mM NaCl and different concentrations of (E) TPP or (F) sodium alginate (Na Alg). All samples were aged 1h at 20 °C before analysis.

Having observed that nanoscale poly(A)-PCMs are stable at physiological ionic strength, we next evaluated their stability over a range of solution pH. Suspensions of **PEG₁₁₃-b-5c₂₇** based poly(A)-PCMs were prepared in PBS buffers ranging from pH 6.0 to 8.0. Between pH 6.0 and 6.8, the poly(A)-PCMs were found to be stable in size with average hydrodynamic diameters of *ca.* 150 to 200 nm (Figure 6c). Between pH 7.3 and 7.7, the poly(A)-PCMs were found to gradually increase in size but remained below *ca.* 250 nm in diameter (Figure 6c). At pH 8.0, the poly(A)-PCMs were found to increase significantly in size to *ca.* 450 nm (Figure 6c) in diameter. Considering that the pK_a values of side-chain ammonium groups in polypeptide **5c** were measured to range between pH 7.5 and 8.0 [52], the ammonium groups of the **5c₂₇** segment will remain mostly charged below pH 7.0, which will favor strong polyelectrolyte complexation with poly(A) in the PCMs and result in minimal size perturbation. As pH increases above pH 7.0 the **5c₂₇** segments will deprotonate and possess lower charge density, which will weaken polyelectrolyte complexation with poly(A) in the PCMs. To study stability of poly(A) complexation at different pH, the RyboGreen assay was used to quantify release of any free poly(A) in solution for poly(A)-PCMs at pH 6.5, 7.3 and 8.3 (Figure 6d). At pH 6.5, we found that the amount of free poly(A) (less than 10%, Figure 6d) was within the range of the poly(A)-PCMs encapsulation efficiency seen above. At pH 7.3, partial deprotonation of side-chain ammonium groups in **5c₂₇** segments occurs, which resulted in a release of nearly 20% of the poly(A) at one hour, which decreased to less than 10% at four hours (Figure 6d). This result may be explained by some poly(A) dissociation and re-complexation occurring over time in these liquid coacervates to achieve stoichiometric PECs as the charge density on **5c₂₇** segments changes. At pH 8.3, significant deprotonation of **5c₂₇** segments occurs and nearly 40% of poly(A) was released (Figure 6d). Overall, above pH 7.3 the loss of cationic charges in **5c₂₇** segments resulted in

destabilization of poly(A)-PCMs and release of poly(A), while over a physiologically relevant pH range of 6.5 to 7.0 the poly(A)-PCMs were found to be generally stable.

An important feature of coacervate core PCMs is their ability to exchange polyelectrolyte chains with those in solution due to the liquid nature of the micelles. Multivalent anionic proteins and polysaccharides are present in intracellular and extracellular environments *in vivo*, and possess the ability to exchange with complexed ssRNA in PCMs resulting in ssRNA release [63–65]. To study how addition of multivalent anions affects poly(A)-PCM stability, model multivalent anions TPP and sodium alginate (Na Alg) were mixed with suspensions of poly(A)-PCMs [66]. First, suspensions of **PEG₁₁₃-b-5c₂₇** based poly(A)-PCMs were mixed with increasing concentrations of TPP and the release of free poly(A) was quantified using the RyboGreen assay (Figure 6e). Note that TPP concentrations of 50 μ M and 250 μ M correspond to 1:1 and 5:1 anion (TPP) to cation (**5c₂₇**) charge ratios, respectively. We observed that *ca.* 20% of complexed poly(A) was released from poly(A)-PCMs within one hour at both TPP concentrations, as compared to less than 10% free poly(A) in 150 mM NaCl without TPP (Figure 6b). These results indicate that TPP is able to exchange with some poly(A) in the poly(A)-PCMs and release it into solution. The similar levels of poly(A) release over a five-fold change in TPP concentration indicate that TPP is only moderately effective in exchanging with poly(A) in the PCMs, likely due its small size and low charge valency compared to the long chain poly(A), which is thus expected to form more stable PCMs with **PEG-b-5c₂₇**.

In order to enhance poly(A) release, suspensions of poly(A)-PCMs were next mixed with increasing concentrations of polymeric Na Alg in the presence of 150 mM NaCl, and the release of free poly(A) was quantified using the RyboGreen assay (Figure 6f). Large excesses of sodium alginate (4.6 and 23 mM) relative to poly(A) (0.025 mM) were used to favor exchange of poly(A) out of the PCMs. However, with 4.6 mM Na Alg, only *ca.* 17% of free poly(A) was released after four hours, and with 23 mM Na Alg *ca.* 40% of free poly(A) was released (Figure 6f). These results showed that poly(A)-PCMs are reasonably stable

against polyanion exchange, but large excesses of polyanions, as may be found in environments *in vivo*, can promote release of free poly(A). Overall, poly(A)-PCMs were found to be stable in aqueous media at physiologically relevant ionic strength, near neutral pH, and in the presence of small molecule, multivalent anions such as TPP. Poly(A) could also be released from poly(A)-PCMs upon exposure to excess polyvalent anions as would be found in intracellular environments. These properties are beneficial for future development of poly(A)-PCMs as nanoscale ssRNA delivery vehicles.

3. Conclusions

Previous studies from our lab demonstrated that cationic, α -helical amino acid side-chain modified poly(S-alkyl-L-homocysteine)s, **5a-5d**, are able to undergo liquid-liquid phase separation at physiologically relevant conditions in aqueous media.⁵¹ Here, these polypeptides were adapted by design of **PEG-b-5b**, and **PEG-b-5c** block copolymers for preparation of spherical, coacervate core PCMs. Variation of polypeptide segment lengths and compositions led to selection of **PEG-b-5c₂₇**, which gave uniform nanoscale PCMs upon mixture with TPP or poly(A) in aqueous media. These PCMs were characterized by DLS, AFM, and cryoEM and were found to be generally stable at physiologically relevant conditions. These model poly(A)-PCMs show promise for future development as ssRNA delivery vehicles. While such vehicles would benefit from cell targeting functionality and functionality to enable endosomal escape, the poly(A)-PCMs have already been shown to encapsulate cargo with high efficiency under biologically compatible conditions and potentially release cargo in the presence of natural polyvalent anions found in intracellular or extracellular environments.

Associated Content

Dedication

This article is dedicated to Fyl Pincus who was an influential mentor at the beginning of my (TJD) independent career. In addition to being an invaluable resource on polymer physics and soft condensed matter, Fyl provided numerous opportunities to join a broader scientific community, constantly livened up our working environment, and is a cherished friend.

Supplementary Information (SI)

The Supplementary Information is available free of charge on the Springer website at DOI: #####.

Methods and experimental procedures, spectral data, additional tables and figures (PDF).

Statements and Declarations

- Funding

This work was supported by NSF (MSN-1807362 and DMR-1904431 to TJD). The authors acknowledge the use of instruments at the Electron Imaging Center for NanoMachines supported by NIH (1S10RR23057) and CNSI at UCLA.

- Competing Interests

None

- Author Contributions

IB, and WAS designed and conducted experiments, analyzed data, and wrote the manuscript.

TJD designed experiments, analyzed data, and wrote the manuscript.

XC and ZHZ collected and analyzed cryoEM data.

• Data Availability Statement: Data for this manuscript is provided in the Supplementary Information file.

References:

1. S. Mitragotri, P. A. Burke, and R. Langer, *Nat. Rev. Drug Discov.* **13**, 655 (2014).
2. T. Friedmann and R. Roblin, *Science* **175**, 949 (1972).
3. R. C. Mulligan, *Science* **260**, 926 (1993).
4. J. R. Bertrand, M. Pottier, A. Vekris, P. Opolon, A. Maksimenko, and C. Malvy, *Biochem. Biophys. Res. Commun.* **296**, 1000 (2002).
5. C. Lorenzer, M. Dirin, A. M. Winkler, V. Baumann, and J. Winkler, *J. Control. Release.* **203**, 1 (2015).
6. K. Kawabata, Y. Takakura, and M. Hashida, *Pharm. Res.* **12**, 825 (1995).
7. S. H. Chen, J. Haam, M. Walker, E. Scappini, J. Naughton, and N. P. Martin, *Curr. Protoc. Neurosci.* **87**, 1 (2019).
8. X. Hou, T. Zaks, R. Langer, and Y. Dong, *Nat. Rev. Mater.* **6**, 1078 (2021).
9. U. Lächelt and E. Wagner, *Chem. Rev.* **115**, 11043 (2015).
10. H. C. Verdera, K. Kuranda, and F. Mingozzi, *Mol. Ther.* **28**, 723 (2020).
11. C. Lonez, M. Vandenbranden, and J. M. Ruyschaert, *Prog. Lipid Res.* **47**, 340 (2008).
12. D. Priftis, K. Megley, N. Laugel, and M. Tirrell, *J. Colloid Interface Sci.* **398**, 39 (2013).
13. D. Priftis, N. Laugel, and M. Tirrell, *Langmuir* **28**, 15947 (2012).
14. H. G. Bungenberg De Jong and H. R. Kruyt, *Proc. K. Ned. Akad. Wet* **32**, 849 (1929).
15. A. N. Singh and A. Yethiraj, *J. Phys. Chem. B* **124**, 1285 (2020).
16. D. V. Krogstad, N. A. Lynd, S. H. Choi, J. M. Spruell, C. J. Hawker, E. J. Kramer, and M. V. Tirrell, *Macromolecules* **46**, 1512 (2013).
17. J. N. Hunt, K. E. Feldman, N. A. Lynd, J. Deek, L. M. Campos, J. M. Spruell, B. M.

- Hernandez, E. J. Kramer, and C. J. Hawker, *Adv. Mater.* **23**, 2327 (2011).
18. E. Spruijt, J. Sprakel, M. A. Cohen Stuart, and J. Van Der Gucht, *Soft Matter* **6**, 172 (2009).
19. D. Priftis, R. Farina, and M. Tirrell, *Langmuir* **28**, 8721 (2012).
20. A. Kawamura, A. Harada, K. Kono, and K. Kataoka, *Bioconjug. Chem.* **18**, 1555 (2007).
21. J. J. Water, M. M. Schack, A. Velazquez-Campoy, M. J. Maltesen, M. Van De Weert, and L. Jorgensen, *Eur. J. Pharm. Biopharm.* **88**, 325 (2014).
22. T. J. Deming, *Prog. Polym. Sci.* **32**, 858 (2007).
23. C. He, X. Zhuang, Z. Tang, H. Tian, and X. Chen, *Adv. Healthc. Mater.* **1**, 48 (2012).
24. H. Lu, J. Wang, Z. Song, L. Yin, Y. Zhang, H. Tang, C. Tu, Y. Lin, and J. Cheng, *Chem. Commun.* **50**, 139 (2014).
25. Y. Shen, X. Fu, W. Fu, and Z. Li, *Chem. Soc. Rev.* **44**, 612 (2015).
26. Y. Liu and L. Yin, *Adv. Drug Deliv. Rev.* **171**, 139 (2021).
27. A. Vaheiri and J. S. Pagano, *Virology* **27**, 434 (1965).
28. F. E. Farber, J. L. Melnick, and J. S. Butel, *Biochim. Biophys. Acta* **390**, 298 (1975).
29. D. Priftis, L. Leon, Z. Song, S. L. Perry, K. O. Margossian, A. Tropnikova, J. Cheng, and M. Tirrell, *Angew. Chem. Int. Ed.* **54**, 11128 (2015).
30. J. Yen, H. Ying, H. Wang, L. Yin, F. Uckun, and J. Cheng, *ACS Biomater. Sci. Eng.* **2**, 326 (2016).
31. J. Yen, Y. Zhang, N. P. Gabrielson, L. Yin, L. Guan, I. Chaudhury, H. Lu, F. Wang, and J. Cheng, *Biomater. Sci.* **1**, 719 (2013).
32. W. Zauner, M. Ogris, and E. Wagner, *Adv. Drug Deliv. Rev.* **30**, 97 (1998).
33. J. S. Kim, B. Il Kim, A. Maruyama, T. Akaike, and S. Wan Kim, *J. Control. Release.* **53**, 175 (1998).
34. Y. Kakizawa, A. Harada, and K. Kataoka, *J. Am. Chem. Soc.* **121**, 11247 (1999).
35. M. Bello Roufaï and P. Midoux, *Bioconjug. Chem.* **12**, 92 (2001).
36. M. A. Bruusgaard-Mouritsen, J. D. Johansen, and L. H. Garvey, *Clin. Exp. Allergy* **51**,

463 (2021).

37. P. Sellaturay, S. Nasser, S. Islam, P. Gurugama, and P. W. Ewan, *Clin. Exp. Allergy* **51**, 861 (2021).

38. A. V. Kabanov, T. K. Bronich, V. A. Kabanov, K. Yu, and A. Eisenberg, *Macromolecules* **29**, 6797 (1996).

39. A. Harada and K. Kataoka, *Macromolecules* **28**, 5294 (1995).

40. A. Harada and K. Kataoka, *Macromolecules* **36**, 4995 (2003).

41. A. E. Marras, T. R. Campagna, J. R. Viereg, and M. V. Tirrell, *Macromolecules* **54**, 6585 (2021).

42. H. M. Van Der Kooij, E. Spruijt, I. K. Voets, R. Fokkink, M. A. Cohen Stuart, and J. Van Der Gucht, *Langmuir* **28**, 14180 (2012).

43. K. Hayashi, H. Chaya, S. Fukushima, S. Watanabe, H. Takemoto, K. Osada, N. Nishiyama, K. Miyata, and K. Kataoka, *Macromol. Rapid Commun.* **37**, 486 (2016).

44. Y. H. Kim, K. Lee, and S. Li, *Chem. Mater.* **33**, 7923 (2021).

45. A. E. Marras, M. Ting, K. C. Stevens, and M. V. Tirrell, *J. Phys. Chem. B* **125**, 7076 (2021).

46. H. Yoon, E. J. Dell, J. L. Freyer, L. M. Campos, and W. D. Jang, *Polymer* **55**, 453 (2014).

47. S. Fukushima, K. Miyata, N. Nishiyama, N. Kanayama, Y. Yamasaki, and K. Kataoka, *J. Am. Chem. Soc.* **127**, 2810 (2005).

48. Z. Ge, Q. Chen, K. Osada, X. Liu, T. A. Tockary, S. Uchida, A. Dirisala, T. Ishii, T. Nomoto, K. Toh, Y. Matsumoto, M. Oba, M. R. Kano, K. Itaka, and K. Kataoka, *Biomaterials* **35**, 3416 (2014).

49. R. J. Christie, Y. Matsumoto, K. Miyata, T. Nomoto, S. Fukushima, K. Osada, J. Halnaut, F. Pittella, H. J. Kim, N. Nishiyama, and K. Kataoka, *ACS Nano* **6**, 5174 (2012).

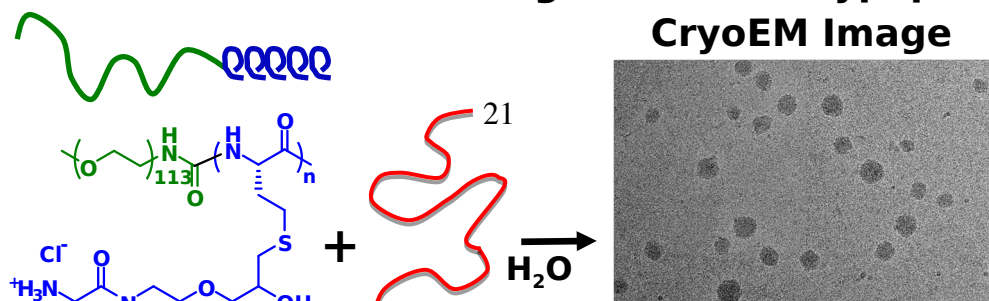
50. C. H. Kuo, L. Leon, E. J. Chung, R. T. Huang, T. J. Sontag, C. A. Reardon, G. S. Getz, M. Tirrell, and Y. Fang, *J. Mater. Chem. B* **2**, 8142 (2014).

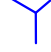
51. H. S. Min, H. J. Kim, M. Naito, S. Ogura, K. Toh, K. Hayashi, B. S. Kim, S. Fukushima, Y.

- Anraku, K. Miyata, and K. Kataoka, *Angew. Chem. Int. Ed.* **59**, 8173 (2020).
52. W. A. Scott, E. G. Gharakhanian, A. G. Bell, D. Evans, E. Barun, K. N. Houk, and T. J. Deming, *J. Am. Chem. Soc.* **143**, 18196 (2021).
53. E. G. Gharakhanian and T. J. Deming, *Chem. Commun.* **52**, 5336 (2016).
54. E. G. Gharakhanian and T. J. Deming, *Biomacromolecules* **16**, 1802 (2015).
55. S. Van Der Burgh, A. De Keizer, and M. A. Cohen Stuart, *Langmuir* **20**, 1073 (2004).
56. J. R. Kramer and T. J. Deming, *Biomacromolecules* **11**, 3668 (2010).
57. S. Tabandeh and L. Leon, *Molecules* **24**, 868 (2019).
58. K. Sadman, Q. Wang, Y. Chen, B. Keshavarz, Z. Jiang, and K. R. Shull, *Macromolecules* **50**, 9417 (2017).
59. X. Yuan, A. Harada, Y. Yamasaki, and K. Kataoka, *Langmuir* **21**, 2668 (2005).
60. M. Lueckheide, J. R. Vieregge, A. J. Bologna, L. Leon, and M. V. Tirrell, *Nano Lett.* **18**, 7111 (2018).
61. J. S. Park, Y. Akiyama, Y. Yamasaki, and K. Kataoka, *Langmuir* **23**, 138 (2007).
62. S. Lindhoud, L. Voorhaar, R. De Vries, R. Schweins, M. A. C. Stuart, and W. Norde, *Langmuir* **25**, 11425 (2009).
63. T. Walimbe and A. Panitch, *Front. Pharmacol.* **10**, 1661 (2020).
64. N. Zheng, L. Yin, Z. Song, L. Ma, H. Tang, N. P. Gabrielson, H. Lu, and J. Cheng, *Biomaterials* **35**, 1302 (2014).
65. N. P. Gabrielson, H. Lu, L. Yin, D. Li, F. Wang, and J. Cheng, *Angew. Chem. Int. Ed.* **51**, 1143 (2012).
66. Y. Xu and F. C. Szoka, *Biochemistry* **35**, 5616 (1996).

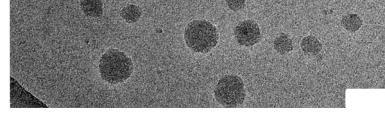
Graphical Abstract:

Coacervate Core PCMs Using α -Helical Polypeptides CryoEM Image




PEG₁₁₃-*b*-5c₂₇
polycation


ssRNA
polyanion



100
nm